

## dc conductivity and the Meyer-Neldel rule in *a*-Si:H

Xiaomei Wang, Y. Bar-Yam,\* D. Adler, and J. D. Joannopoulos

Center for Materials Science and Engineering, Massachusetts Institute of Technology, Cambridge, Massachusetts 02139

(Received 4 April 1988)

Disorder in amorphous semiconductors results in unusual properties of dc conductivity. We demonstrate a quantitative description of the temperature dependence of conductivity in *a*-Si:H. The universal activation energy dependence of the conductivity prefactor (the Meyer-Neldel rule) is reproduced. Excellent agreement with experimental results is obtained by describing disorder and defects using the general thermodynamic ensemble theory for the structure of disordered systems.

Hydrogenated amorphous silicon (*a*-Si:H) has been intensively studied in recent years. In comparison with crystalline semiconductors, *a*-Si:H exhibits certain new features. One of them is dc conductivity. Unlike crystalline semiconductors, for which the Arrhenius plot is a straight line, *n*-type doped *a*-Si:H shows a kink at a temperature around 400 K.<sup>1</sup> Just below the kink temperature, the Arrhenius plot possesses a concavity which was most clearly indicated in recent experiments.<sup>2</sup> We display a typical experimental plot<sup>1</sup> in Fig. 1. While possessing these unique features, *a*-Si:H exhibits a more important universal property of the conductivity, known as the Meyer-Neldel rule:<sup>3</sup>

$$\sigma_0 = \sigma_{00} \exp(E_a/k_B T_0). \quad (1)$$

Here,  $\sigma_0$  is the extrapolation of the Arrhenius plot from room temperature to  $T = \infty$ . The associated slope defines the activation energy  $E_a$ .  $\sigma_{00}$  and  $T_0$  are constants for a given material. This relation unifies the behavior of

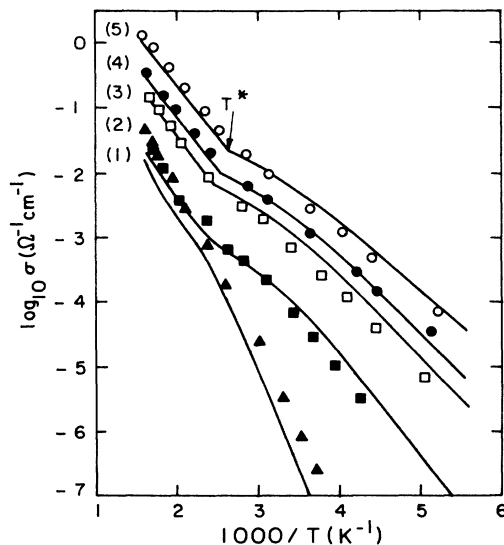


FIG. 1. Comparison of the experimental (Ref. 1) and theoretical Arrhenius plot for various doping levels of phosphorus-doped *a*-Si:H. (1) 1 ppm, (2) 3 ppm, (3) 250 ppm, (4) 1000 ppm, and (5) 10000 ppm.

different samples prepared under different conditions and has been universally observed in various kinds of disordered systems, inhomogeneous semiconductors, and organic semi-insulators.<sup>4</sup>

A number of theoretical models have been proposed to explain the interesting properties of conductivity. For example, the kink for *n*-type *a*-Si:H has been described within the two-path conduction model<sup>5</sup> and the compensation model.<sup>6</sup> More recent detailed experiments<sup>2</sup> have attributed it to a transition of structural equilibrium above the kink temperature. The Meyer-Neldel rule has been investigated in the thermally assisted tunneling model.<sup>7</sup> The idea of a disorder-induced shift of the Fermi energy<sup>8,9</sup> has also been suggested. However, to date no theory has successfully given a quantitative description which is in agreement with measurements.

In this paper, we use the general thermodynamic-ensemble theory for disordered systems<sup>10</sup> to model the electronic structure, and use the extended state conduction model to describe the transport of carriers in *a*-Si:H. We provide a quantitative analysis of the properties of the Fermi energy, the temperature dependence of dc conductivity, and the Meyer-Neldel rule. The theoretical results are in excellent agreement with experiments.

In the temperature regime we are interested in, electronic transport in amorphous solids is likely to be dominated by extended states. Therefore, the Greenwood formula<sup>11</sup> provides

$$\sigma(T) = \int \mu(\epsilon, T) g(\epsilon, T) f(\epsilon, T) d\epsilon, \quad (2)$$

where  $\mu(\epsilon, T)$ ,  $g(\epsilon, T)$ , and  $f(\epsilon, T)$  are the mobility, density of states, and Fermi-Dirac distribution function, respectively. We further assume that the mobility  $\mu(\epsilon, T)$  is a constant  $\mu_0$  for all extended states  $\epsilon > \epsilon_c$ , and that it vanishes for  $\epsilon < \epsilon_c$  ( $\epsilon_c$  is the conduction mobility edge). Thus, we focus on the properties of the electronic density of states and the Fermi energy.

The central point of the thermodynamic-ensemble theory is that the amorphous solid structure itself is determined by the formation free energy of deviations from the effective ground state—an ideally bonded network. This theory assumes that there exists a freezing temperature  $T^*$ , above which both structural and electronic equilibrium can be reached, but below which the structure is

frozen. Thus, when  $T > T^*$ , the defects with formation energy  $F_d$  have the number density  $N_d = N_0 \exp(-F_d/k_B T)$ .  $N_0$  is the associated atomic density. When  $T < T^*$ , the total defect number of one type is fixed, e.g., for a defect which can exist in three charge states,  $N_d = N_d^+ + N_d^0 + N_d^-$  is fixed. The formation energy of a defect in a charged state is Fermi energy dependent. As the Fermi energy rises the negative (positive) defects become lower (higher) in energy. For a three-charge-state defect,

$$F_{d-} = F_{d^0} + \epsilon_d(0/-) - \mu,$$

$$F_{d+} = F_{d^0} - \epsilon_d(+/0) + \mu,$$

while for a two-charge-state phosphorous impurity

$$F_{p+} = F_{p^0} - \epsilon_p(+/0) + \mu.$$

Here,  $\epsilon_d(0/-)$ ,  $\epsilon_d(+/0)$ , and  $\epsilon_p(+/0)$  represent thermodynamic transition energies defined as the position of the Fermi energy at which the defect energies in the two different charge states are the same. The effective correlation energy is determined by  $U = \epsilon_d(0/-) - \epsilon_d(+/0)$ . In principle, the freezing temperature has a complex dependence on the properties of the defects as well as the experimental conditions. For different types of defects,  $T^*$  is not necessarily the same.

Applied to  $a$ -Si:H, this model has qualitatively explained the properties of band tails, dangling-bond defect states, and the doping dependence of the Fermi energy.<sup>10</sup> In our calculation, we again consider bands, band tails, intrinsic three-charge-state defects, and phosphorus dopants. We assume zero correlation energy and one single freezing temperature for both intrinsic defects and phosphorus defects. The modification of  $T^*$  by the doping is given by the simple form<sup>10,12</sup>

$$T^* = T_0^* - a \log_{10}[N(p) + 1],$$

where  $N(p)$  measures the doping level in ppm,  $T_0^*$  and  $a$  are independent of the doping, and are deduced from experimental data.<sup>1,2</sup> The bands can be conveniently chosen to have the Tauc form  $g_c(\epsilon) = A_c \sqrt{\epsilon - \epsilon_c^i}$  for  $\epsilon > \epsilon_c$  and  $g_v(\epsilon) = A_v \sqrt{\epsilon_v^i - \epsilon}$  for  $\epsilon < \epsilon_v$ , where  $\epsilon_c^i - \epsilon_v^i$  is the Tauc optical gap. The band tails have exponential forms (Refs. 10 and 13)  $g_{ct}(\epsilon) = A_{ct} \exp[(\epsilon - \epsilon_c)/k_B T_c]$  and  $g_{vt}(\epsilon) = A_{vt} \exp[-(\epsilon - \epsilon_v)/k_B T_v]$ , where  $T_c = T_c^0$ ,  $T_v = T_v^0$  (for  $T < T^*$ ), and  $T_c = (T_c^0/T^*)T$ ,  $T_v = (T_v^0/T^*)T$  (for  $T > T^*$ ). Defect states are chosen to have Gaussian distributions. Table I is the summary of input constants used in the evaluation of the density of states. There, the mobility gap, the Tauc optical gap,  $T_c^0$ ,  $T_v^0$ , and  $T_0^*$  are chosen directly from experiments, while constant  $A_c$  ( $A_v$ ) is determined by the density of states at the joining point  $\epsilon_c$ ,  $N_c(\epsilon_c) \sim 3 \times 10^{21} \text{ eV}^{-1} \text{ cm}^{-3}$ ; the peak position of transition energy for the intrinsic defect is determined by the Fermi energy of undoped material which is 0.6 eV below the conduction mobility edge; the peak of the phosphorus impurity level is  $\sim 0.1$  eV below  $\epsilon_c$ ; the formation free energies  $F_d^0$  and  $F_p^0$  are calculated from the measurements  $n(e)/n(D^-) \sim 10^{-1}$ ;  $n(D^-)/[n(p)n(\text{si})] \sim 10^{-7}$  (see Ref. 10). In Fig. 2 we display the density of states together

TABLE I. Collection of input constants used in the evaluation of the density of states.

CV bands	$\epsilon_c = -\epsilon_v = 0.9$ eV, $\epsilon_c^i = -\epsilon_v^i = 0.87$ eV $A_c = A_v = 8 \times 10^{21} (\text{cm}^{-3} \text{eV}^{-1})$
Freezing temp. (K)	$T_0^* = 440$ , $a = 15$
Band tails (K)	$T_c^0 = 325$ , $T_v^0 = 500$
Intrinsic defect	$N_0 = 5 \times 10^{22} (\text{cm}^{-3} \text{eV}^{-1})$ , $F_d^0 = 0.75$ eV $\epsilon_d$ , peak: 0.3 eV; width: 0.15 eV
Phosphorus constants (eV)	$F_p^0 = 0.48$ $\epsilon_p(+/0)$ , peak: 0.8; width: 0.04

with the shallow states of a few typical cases in our model. It is in general agreement with the experimental data.<sup>14</sup>

Having the knowledge of the density of states determined by experimental data and our model, the Fermi energy as a function of any quantity related to our model

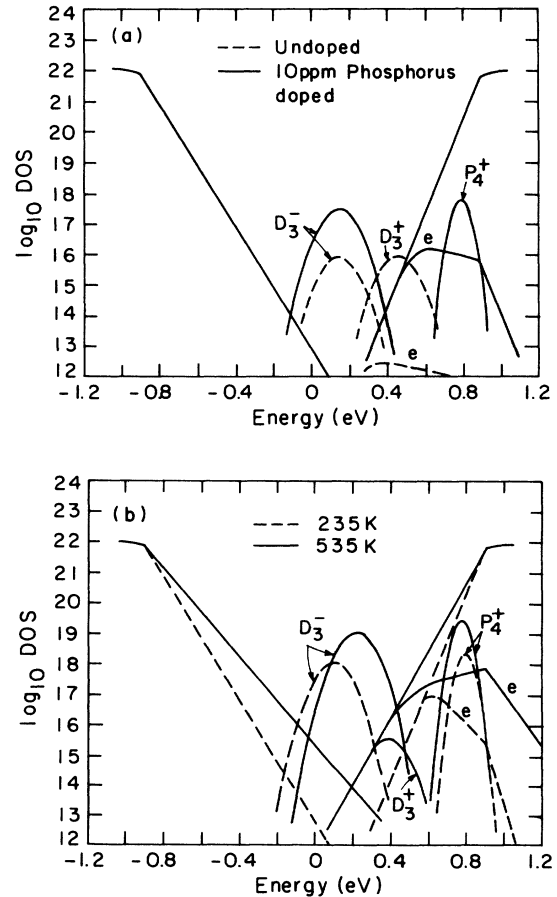


FIG. 2. The density of states of  $a$ -Si:H. (a) At 300 K: dashed line for undoped samples and solid line for 10-ppm phosphorus-doped samples. (b) 1000-ppm phosphorus-doped samples: dashed line for  $T < T^*$  and solid line for  $T > T^*$ .

can be calculated self-consistently from the charge neutrality,

$$n(e^-) + n(D^-) = n(h^+) + n(D^+) + n(P_4^+).$$

We obtain the dc conductivity by using Eq. (2) where  $\mu_0$  is the only fitting parameter. We assume that the atomic concentration of dopant atoms in the solid phase  $C_{\text{sol}}$  is the same as that in the gas phase  $C_{\text{gas}}$ .<sup>15</sup> Finally, we approach the problem of understanding the physics behind the Meyer-Neldel rule by isolating the various components that give rise to the complexity associated with the experimental conditions. In order to draw out the general features, we consider several intrinsic physical quantities *independently*: doping level, freezing temperature  $T^*$ , dopant formation energy, and transition energies. Our results are presented and discussed below. We begin with the dc conductivity.

**dc conductivity.** The temperature dependences of the dc conductivity for different doping levels are plotted in Fig. 1 together with the experimental data. The agreement is excellent with the fitting parameter  $\mu_0 = 50(\text{cm}^2\text{V}^{-1}\text{s}^{-1})$ . The fitting mobility is somewhat larger than the experimental value  $\sim 10(\text{cm}^2\text{V}^{-1}\text{s}^{-1})$ .<sup>13</sup> This deviation should be reduced if we take into account the differences between  $C_{\text{sol}}$  (usually higher<sup>15</sup>) and  $C_{\text{gas}}$ . Since the Fermi energy plays an essential role in determining electronic transport properties, we discuss it first. For various doping levels, the overall behavior of the Fermi energy as a function of temperature (see Fig. 3) is striking. A kink is observed at  $T = T^*$ . For "impure" materials, at temperature below  $T^*$ , the dominant charged defects are  $P_4^+$  and  $D^-$ . The charge neutrality condition can be approximately written as  $n(e^-) + n(D^-) \cong n(P_4^+)$ . Since the number of  $D^-$  and  $P_4^+$  states are frozen out for  $T < T^*$ , as the temperature increases the Fermi level has to decrease to satisfy the charge neutrality condition. This decrease goes faster as  $T$  goes higher.<sup>16</sup> For  $T > T^*$ ,  $n(D^-)$  and  $n(P_4^+)$  increase as  $\exp(-F_d^-/k_B T)$  and  $\exp(-F_p^+/k_B T)$ , respectively.  $n(P_4^+)$  will increase faster than  $n(D^-)$  because

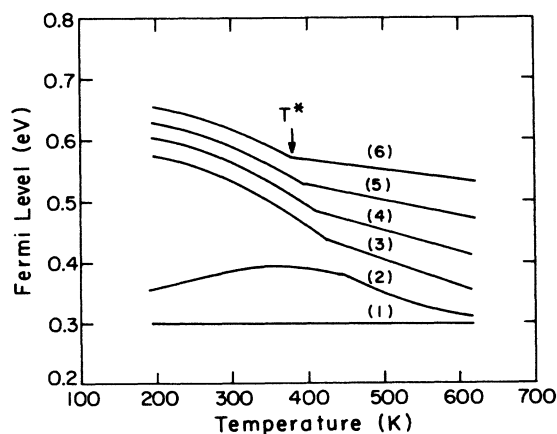


FIG. 3. The Fermi energy as a function of temperature for different doping levels (1) undoped, (2) 1 ppm, (3) 10 ppm, (4) 100 ppm, (5) 1000 ppm, and (6) 10000 ppm.

the formation energy of  $P_4^+$  is smaller than that of  $D^-$  according to our model. This results in a slower decrease of the Fermi energy for  $T > T^*$ . We believe this is the origin of the kink in the  $\mu$  vs  $T$  curve at  $T = T^*$ . [We point out here that a similar behavior is actually observed for Li-doped *a*-Si:H (Ref. 1).] Full understanding of the temperature dependence of the Fermi energy leads us to a clear interpretation of the conductivity behavior shown in Fig. 1. At low temperature, the Arrhenius plot is linear, because the dependence of the Fermi energy on temperature is weak. As  $T$  approaches  $T^*$ , it becomes concave. The concavity corresponds to the faster drop in the Fermi energy (see Fig. 3). When the temperature is above the freezing temperature,  $\ln\sigma$  is linear with  $T$  since the Fermi level decreases linearly with  $T$  in this temperature region. The larger activation energy for  $T > T^*$  (compared with that for  $T < T^*$ ) results from the smaller statistical shift of the Fermi level (compared with that for  $T < T^*$ ).

We conclude that the temperature dependence of the Fermi energy completely accounts for the properties of the dc conductivity. In particular, the discontinuity of the Fermi energy which arises because of changes in structural relaxation processes is responsible for the kink that appears in the Arrhenius plot.

**Meyer-Neldel rule.** Motivated by the results just described, we next study the physics behind the Meyer-Neldel rule by describing the effects of the amorphous nature of materials on the dc conductivity. We present the theoretical and experimental<sup>17</sup> results of  $\sigma_0$  as a function of the activation energy in Fig. 4. The extrapolation is carried out by fitting the computer data of the Arrhenius plot linearly in the range of 220–320 K. The theoretical

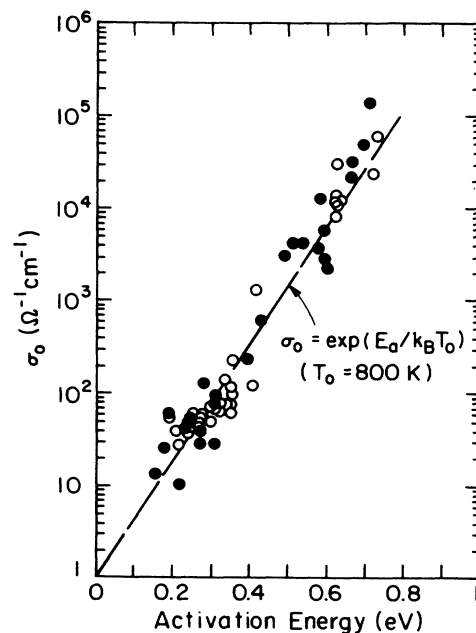


FIG. 4. The preexponential factor  $\sigma_0$  as a function of the activation energy. (O) Theory and (●) experimental data (Ref. 17). The theoretical data are obtained by varying doping level, transition energies, formation free energies, and freezing temperature independently.

results are an accumulation of calculated data obtained by varying independently doping level, transition energies, formation free energies, and freezing temperature. In the plot, we do not explicitly distinguish between the variety of theoretical data as we are only concerned with their general behavior. However, we discuss a few typical cases below. When the doping level is varied systematically from 0.1 to 10000 ppm, the activation energy decreases from 0.62 to 0.18 eV and the scattered data fall along the line given by Eq. (1) with  $T_0 \sim 800$  K,  $\sigma_{00} = 1 \Omega^{-1} \text{cm}^{-1}$ . However, the data do not spread over the entire range uniformly. A cluster locates in the region of  $E_a \sim 0.19$  to 0.35 eV, while a few points representing the lightly doped samples group around  $E_a \sim 0.61$  eV. This behavior is directly related to the properties of the Fermi energy dependence on doping. Both the experiments<sup>18</sup> and our study show that there is a jump in the Fermi energy in a very narrow range of doping levels at low temperature, which we believe is due to the competition between the  $D^+$  and  $P_4^+$  states. The data for smaller transition energy of the intrinsic defect are also presented. The activation energy is in the range from 0.25 to 0.72 eV. Changing the

dopant formation energy and transition energy is equivalent to changing the dopant itself in this model. The behavior is similar to that of the phosphorus dopant. More surprisingly, the data obtained by varying the freezing temperature from 350 to 520 K (this could mean varying the substrate temperature or perhaps hydrogen content in real samples) also obey the same relation. For the high concentration of dopant, the lower freezing temperature gives the larger activation energy, while for the low concentration of dopant, the higher freezing temperature produces the larger activation energy. We emphasize that  $\mu_0$  is kept constant as we change the other variables.

In summary, we provide a quantitative description of the properties of the dc conductivity and Meyer-Neldel rule in *a*-Si:H in our model. We find that the behavior of the Fermi energy is primarily responsible for the nature of defect states, doping, and transport.

This work was supported in part by U.S. Office of Naval Research Contract No. N00014-86-K-0158, and the Solar Energy Research Institute under Contract No. DE-AC02-83CH10093.

\*Also at IBM Thomas J. Watson Research Center, Yorktown Heights, NY 10598. Current address: Materials Research Department, Weizmann Institute of Science, Rehovot, Israel.

<sup>1</sup>W. Beyer and H. Overhof, in *Semiconductors and Semimetals: Hydrogenated Amorphous Silicon, Pt. C: Electronic and Transport Properties*, edited by R. K. Willardson and A. C. Beer (Academic, Orlando, 1984), p. 257.

<sup>2</sup>J. Kakalios and R. A. Street, *Phys. Rev. B* **34**, 6014 (1986); R. A. Street, J. Kakalios, and T. M. Hayes, *ibid.* **34**, 3030 (1986).

<sup>3</sup>W. Meyer and H. Neldel, *Z. Tech. Phys.* **18**, 588 (1937).

<sup>4</sup>G. G. Roberts, *Phys. Rep.* **60**, 59 (1980).

<sup>5</sup>Z. S. Jan, R. H. Bube, and J. C. Knights, *J. Electron. Mater.* **8**, 47 (1979); D. A. Anderson and W. Paul, *Philos. Mag. B* **45**, 1 (1982).

<sup>6</sup>R. A. Street, *J. Non-Cryst. Solids* **77/78**, 1 (1985).

<sup>7</sup>G. Kemeny and B. Rosenberg, *J. Chem. Phys.* **52**, 4151 (1970); **53**, 3549 (1970); G. G. Roberts, *J. Phys. C* **4**, 3167 (1971).

<sup>8</sup>F. R. Shapiro and D. Adler, *J. Non-Cryst. Solids* **66**, 303 (1984).

<sup>9</sup>H. Fritzsche, *Sol. Energy Mater.* **3**, 417 (1980).

<sup>10</sup>Y. Bar-Yam, D. Adler, and J. Joannopoulos, *Phys. Rev. Lett.* **57**, 467 (1986).

<sup>11</sup>O. Madelung, *Introduction to Solid-State Physics* (Springer-Verlag, Berlin, 1978).

<sup>12</sup>Y. Bar-Yam, D. Adler, and J. Joannopoulos, in *MRS Spring Meeting, 1987* (unpublished).

<sup>13</sup>See T. Tiejie, in Ref. 1, p. 207.

<sup>14</sup>J. Kocka, *J. Non-Cryst. Solids* **90**, 91 (1987).

<sup>15</sup>For glow-discharged *a*-Si:H, this is likely to be true. See M. Stutzmann, D. K. Biegelsen, and R. Street, *Phys. Rev. B* **35**, 5666 (1987).

<sup>16</sup>We can prove that this decrease approximately goes  $\sim T^2$ .

<sup>17</sup>D. E. Carlson and C. R. Wronski, *Amorphous Semiconductors*, Topics in Applied Physics, Vol. 36 (Springer-Verlag, Berlin, 1979).

<sup>18</sup>W. E. Spear and P. G. LeComber, *Philos. Mag.* **33**, 935 (1976).